

RESEARCH ARTICLE

# Immunohistochemical biomarkers and distribution of telocytes in ApoE<sup>-/-</sup> mice

Ying Xu<sup>1</sup>, Hu Tian<sup>1\*</sup>, Jialin Cheng<sup>2</sup>, Shubin Liang<sup>2</sup>, Teng Li<sup>2</sup> and Ju Liu<sup>3</sup>

<sup>1</sup> Department of General Surgery, Shandong Provincial Qianfoshan Hospital, Shandong University, Jinan, Shandong, People's Republic of China

<sup>2</sup> Taishan Medical University, Tai'an, Shandong, People's Republic of China

<sup>3</sup> Medical Research Center, Shandong Provincial Qianfoshan Hospital, Shandong University, Jinan, Shandong, People's Republic of China

## Abstract

Telocytes had been identified as a peculiar stromal cell type implicated in tissue homeostasis and the development and pathophysiology of diseases. Telocyte existed in most organs and tissues in humans and animals. However, few studies have examined telocytes in ApoE gene deficient mice. In our studies, we verified the existence, the morphology and immunohistochemical characteristics of telocytes in critical organs of the ApoE<sup>-/-</sup> mice. Male adult ApoE<sup>-/-</sup> mice were selected as an experimental model. Immunohistochemical bio-markers, such as CD34, CD117, CD28, Vimentin and PDGFR- $\alpha$  were utilized to determine the distribution and morphology of telocytes in the heart, liver and kidney. Telocyte expressed positively for CD34 and CD117, and partial telocyte and telopode expressed positively for PDGFR- $\alpha$  in heart and liver, but negatively in kidney. Double immunofluorescence assays for CD28/Vimentin, CD34/CD117 and CD34/PDGFR- $\alpha$  were used to demonstrate the biochemistry speciality of telocytes, respectively. The evidence of telocytes in the ApoE<sup>-/-</sup> mice is the first step of our study, which aims to demonstrate changes in telocytes in atherosclerosis in this animal model.

**Keywords:** ApoE<sup>-/-</sup> mice; CD28; CD34; Telocyte; Telopode

## Introduction

Telocytes, a type of stromal cell, are present in humans and various animals and are distinct from 'interstitial cells of Cajal' (ICC) in terms of ultrastructure, immunohistochemical bio-markers, gene expression and protein profiles. Telocytes were discovered by various modern techniques and first described by Popescu (Nicolescu and Popescu, 2012). Telocytes have a small-sized and irregular body with several extremely long, thin and moniliform-like telopodes (Tps), which possess alternating regions of podomers and podoms (250–300 nm) (Rusu et al., 2012; Zheng et al., 2012; Cantarero et al., 2011; Gherghiceanu et al., 2008). Tps are considered an important channel for transporting information, connecting with homocellular or heterocellular junctions, and establishing three-dimensional

networks. Based on their distribution, telocytes have been proposed to participate in a wide range of physiological and pathological processes, such as the maintenance of tissue homeostasis, regeneration, cell proliferation and intercellular signalling. Furthermore, telocytes are known to exert their functions via direct intercellular connections or through the secretion of extracellular vesicles and exosomes (Alunno et al., 2015). Using horse and pig animal models to study the development of atrial fibrillation and cardiac diseases (Bode et al., 2015; Declodt et al., 2015), Vandecasteele produced a 3D image of telocytes in pulmonary veins (Vandecasteele et al., 2018). A few studies have reported that immunohistochemical staining and light microscopy techniques can be used to quantify the morphology of telocytes in various systems of humans and different animals.

\*Corresponding author: e-mail: tianhu6585@163.com

**Abbreviations:** ApoE<sup>-/-</sup>, ApoE gene deficiency; EDTA, Ethylenediaminetetraacetic acid; ICC, Interstitial cells of Cajal; IF, Immunofluorescence; IHC, immunohistochemistry; PDGFR- $\alpha$ , Platelet-derived growth factor receptor - $\alpha$ ; TCs, Telocytes; TEM, Transmitted electron microscopy; Tps, Telopodes

-----  
This is an open access article under the terms of the Creative Commons Attribution-NonCommercial-NoDerivs License, which permits use and distribution in any medium, provided the original work is properly cited, the use is non-commercial and no modifications or adaptations are made.

**Table 1** Immunohistochemistry labels

IHC bio-marker	Heart	Liver	Kidney	Primary antibody Dilution rate	Producer and number
CD34	√	√	√	1:3000	Abcam AB81289
CD28	√	-	-	1:200	Abcam AB203084
CD117	√	√	√	1:500	Servicebio GB11073
Vimentin	√	-	√	1:1000	Servicebio GB11192
PDGFR- $\alpha$	√	√	√	1:200	Servicebio GB11261

Mark '√' in the column expresses which bio-mark is selected to be stained. Mark '-' in the column expresses untested bio-mark. Liver organ is stained by Rabbit Primary antibodies-CD34, CD117 and PDGFR- $\alpha$ ; Kidney is stained by Rabbit Primary antibodies-CD34, CD117, Vimentin and PDGFR- $\alpha$ ; Heart organ is stained with antibodies-CD34, CD117, CD28, Vimentin and PDGFR- $\alpha$ . The second antibody is Caprine anti-Rabbit HRP for different dilutions followed.

ApoE<sup>-/-</sup> mice are prone to atherosclerosis under high fat diets. These mice models can simulate similar atherosclerotic pathological processes in the arteries of humans (Nakashima *et al.*, 1994). The ApoE<sup>-/-</sup> mice model has been utilized and accepted in numerous studies worldwide for the study of atherosclerosis (Yang *et al.*, 2016). Medical research on human and normal mice has already considered telocyte histology and pathology; however, telocytes have yet to be studied in ApoE<sup>-/-</sup> mice. Recent telocyte studies have found interesting functional telocyte morphology in various organs and have also discovered potential significant roles of telocytes in abnormal gene animal models. However, studies on telocyte immunophenotypes have primarily focused on single immunohistochemical bio-markers, such as CD34, CD117 or Vimentin. The lack of appropriate antibodies for these immunohistochemical assays have limited our ability to confirm the functions and characteristics of telocytes. To identify the morphology and immunophenotypes of telocytes in ApoE<sup>-/-</sup> mice, three immunohistochemical antibodies were used to examine the expression profiles of CD28 and platelet-derived growth factor- $\alpha$  (PDGFR- $\alpha$ ) (Table 1).

## Methods and materials

### Animal preparation

Ten male ApoE<sup>-/-</sup> mice (identification number: SCXK2016-0006, Beijing Vital River Laboratory Animal Technology Co., Ltd., China), ranging from 56-68-days-old

and 18 g – 23 g were utilized in our study (Medical Research Centre and Laboratory Animal Centre, Shandong Provincial Qianfoshan Hospital, Shandong University). The mice were housed at 22°C under a 12-hour light/12 hour dark cycle and fed a high fat diet for 6 weeks with free access to tap water in the Medical Research Centre of Shandong Provincial Qianfoshan Hospital.

### Samples preparation

Briefly, after each mouse was weighed, 10% chloral hydrate solution was used to anesthetise the ApoE<sup>-/-</sup> mice (0.004 ml/g body weight) through intraperitoneal injection. The mice were then fixed in a supine position with their necks extended. A median incision to the abdomen was made to open the abdominal cavity and then the thoracic cavity to harvest organs in the following sequence: liver, kidney and heart. Organs were fixed in 4% buffered paraformaldehyde solution, embedded in paraffin using paraffin embedding machine JB-P5 (Junjie Electro Co., Wuhan, China) and archived. Then, 3- $\mu$ m thick sample tissue sections were prepared using pathology slicer RM2016 (Laika Alliance Co. of Shanghai, USA). The sections were sequentially washed in triplicate in xylene (15 min each), dehydrated twice in pure ethanol (5 min each), and dehydrated in an ethanol gradient of 85% and 75% (5 min each). The sections were incubated in sodium citrate antigen retrieval solution (Servicebio: G1202, pH 6.0) and washed 3 times with PBS (Servicebio: G0002, pH 7.4) on a rocker device (Servicebio: TSY-B, Germany) for 5 min per wash. Objective tissues were marked with a liquid blocker pen (Gene tech: GT1001, China) and soaked in 3% BSA (Servicebio: G5001, China) at room temperature for 30 min.

### Immunohistochemistry assay

Single label immunohistochemical assays were performed using primary antibodies for specific biomarkers (Table 1). Sample slides were incubated with the appropriate primary antibodies overnight at 4°C and subsequently labelled with secondary antibody (Caprice anti-rabbit, G23303, 1:200 dilution, from Servicebio, China) and HRP at room temperature for 50 min (Servicebio: G1211). The slides were then dried, and freshly prepared DAB chromogenic reagents were used to label the marked tissue. Reaction times were monitored by microscopy until cell nuclei showed a brown-yellow colour. Nuclei were counterstained with haematoxylin staining solution (G1004, Servicebio Cor, USA). The slides were then treated with the differentiation solution (G1039, Servicebio Cor, USA) for a few seconds and washed under running tap water. Then, the slides were treated with a bluing solution (G1040, Servicebio Cor, USA) and washed under running tap water.

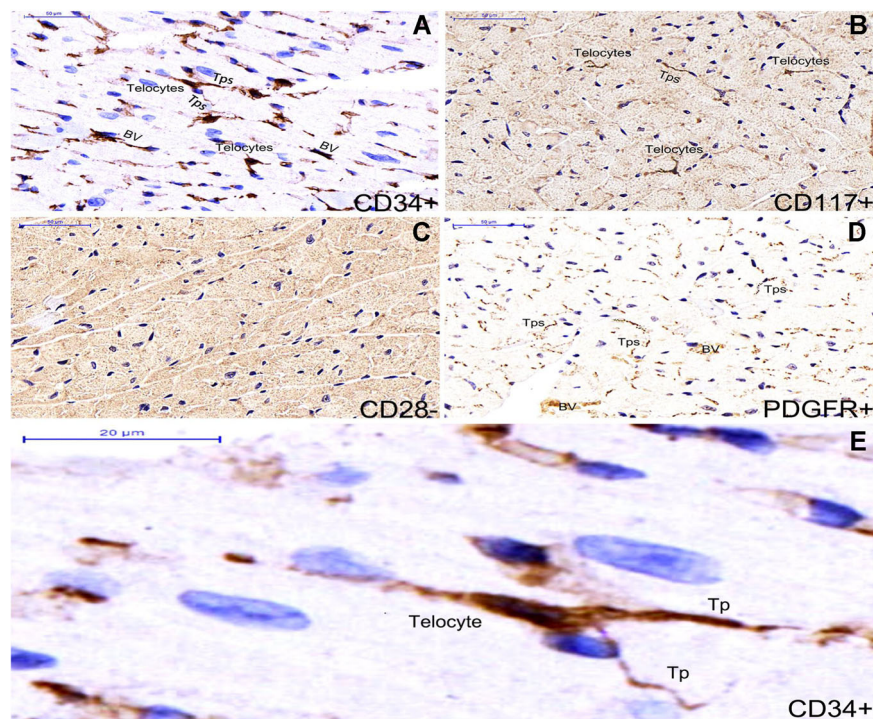


**Figure 1** Single staining immunohistochemistry by different bio-markers in myocardium tissue of ApoE<sup>-/-</sup> mice and distinct morphological types of telocytes are shown (A-E). Telocytes expressed positively for CD34 (A) and CD117 (B), meanwhile telopods of telocyte expressed positively for PDGFR- $\alpha$  (D). Telocytes are shown negatively for CD28 bio-marker (C). CD34<sup>+</sup> telocyte with three long and thin telopods is shown between myocardial cells. BV : blood vessel (A). Nuclei were counterstained with haematoxylin(blue). The scale bar = 50 $\mu$ m( A-D) and 20 $\mu$ m (E).

Positive cells as identified by DAB reagent (G1211, Servicebio Cor., USA) showed brown-yellow nuclei.

Overall, 16 distinct single-stained bio-marker samples from 3 organs were evaluated by microscopy. Images were captured (Microscope Camera XSP-C204, Olympus Europa GmbH, Hamburg, Germany) at a magnification of 400  $\times$  at 300 dpi in TIFF format. Photoshop software was used to false-colour fluorescent markers in the images.

### Immunofluorescence assay

All sections were incubated in 2 changes of xylene at 15 min each. A dehydrator (JJ-12J, Junjie electronic corporation of Wuhan, China) was used to dehydrate the sections in 2 changes of pure ethanol (from Shanghai Clinical Research Center, SCRC, China) at 5 min each, followed by dehydration in an ethanol gradient of 85% and 75%, respectively, at 5 min each. Then, the slides were immersed in EDTA antigen retrieval buffer (pH 8.0, G1206, Servicebio Cor, USA) at a sub-boiling temperature for 8 min, let stand for 8 min, and followed by another sub-boiling incubation for 7 min. The slides were washed three times with PBS (pH 7.4) on a rocker device (TSY-B, Servicebio Cor, USA) at 5 min each. Liquids were removed from the superficial sections, and the objective tissue were

marked with a liquid blocker pen (GT1001, Gene tec., China). A fluorescence quenching reagent (G1221, Servicebio Cor., USA) was added and the slides were incubated for 5 min. Then, the slides were incubated with primary antibodies to double stain for CD34/CD117, CD28/Vimentin, or CD34/PDGFR- $\alpha$  (diluted with PBS) overnight at 4 $^{\circ}$ C in a wet box containing water. Subsequently, the slides were incubated with secondary antibody after washing three times with PBS (pH 7.4) on a rocker device for 5 min each. The objective tissue was covered with the secondary antibody and incubated at room temperature for 50 min in the dark. Then, the slides were incubated with DAPI (G1012, Servicebio Cor, USA) at room temperature for 10 min. The slides were washed three times with PBS (pH 7.4) on a rocker device for 5 min each. Then, samples were mounted with a coverslip (10212432 C, CITOTEST, Berlin, Germany) and anti-fade mounting medium (G1401, Servicebio Cor, USA). The samples were viewed by microscopy and images were collected using fluorescence microscopy (Nikon Eclipse C1, Tokyo, Japan) with an imaging system (Nikon DS-U3, Tokyo, Japan). DAPI was confirmed using a UV excitation wavelength of 330-380 nm and an emission wavelength of 420 nm. FITC was captured by an excitation wavelength of 465-495 nm

and an emission wavelength of 515-555 nm. CY3 was captured by an excitation wavelength of 510-560 nm and an emission wavelength of 590 nm. Nuclei were labelled with DAPI. Positive cells were green or red based onto the fluorescent label used. Images were captured at 1 to 400 $\times$  magnification (Microscope Camera XSP-C204, Olympus Europa GmbH, Hamburg, Germany).

## Results

Single labelling immunohistochemistry for CD34, CD117, CD28, PDGFR- $\alpha$  and double labelling immunofluorescence for CD28/Vimentin, CD34/CD117, CD34/PDGFR- $\alpha$  were simultaneously used to identify the morphology and distribution of telocyte in the heart, liver and kidney of ApoE<sup>-/-</sup> mice. Different scale bars are shown with the same marker to make the morphology of telocyte and telopode more explicitly.

### In heart organ

Telocytes with telopodes express positively for CD34 and CD117 (Figure 1A,B,E). Telocyte morphology is dependent on the number of telopodes extending from the telocyte body. PDGFR- $\alpha$  is expressed positively in the prolonged

and thin telopodes (Figure 1A-D). Telocytes are negative in immunohistochemistry assays for CD28 (Figure 1A-C). Telocytes with telopodes are positive for CD34 and form a 3D network among myocardial cells as indicated by double immunofluorescence labelling for CD34/PDGFR- $\alpha$  (Figure 2A-C) and telopodes can be easily distinguished (Figure 2D-F).

### In kidney organ

Telocytes are positive for CD34 and PDGFR- $\alpha$ , and negative for CD117 in the cortex system and medulla nephrica system of kidney (Figures 3 and 4). Their morphologies are similar in the two systems (Figure 3A-F,G). Cells in the cortex system and medulla nephrica system of renal tissues are extensively stained by double immunofluorescence labels for CD28 and Vimentin, but there is no evidence of telocyte shown obviously (Figure 4G,H,I). Double staining immunofluorescence labels CD34/PDGFR- $\alpha$ -positive telocyte is spindle-like with two telopodes (Figure 4A-D,E,F), and telocytes construct a network (Figure 4A-C).

### In liver organ

Telocytes are expressed positively for CD34 and CD117 (Figure 5A,B,D), and telopodes are positive for PDGFR- $\alpha$

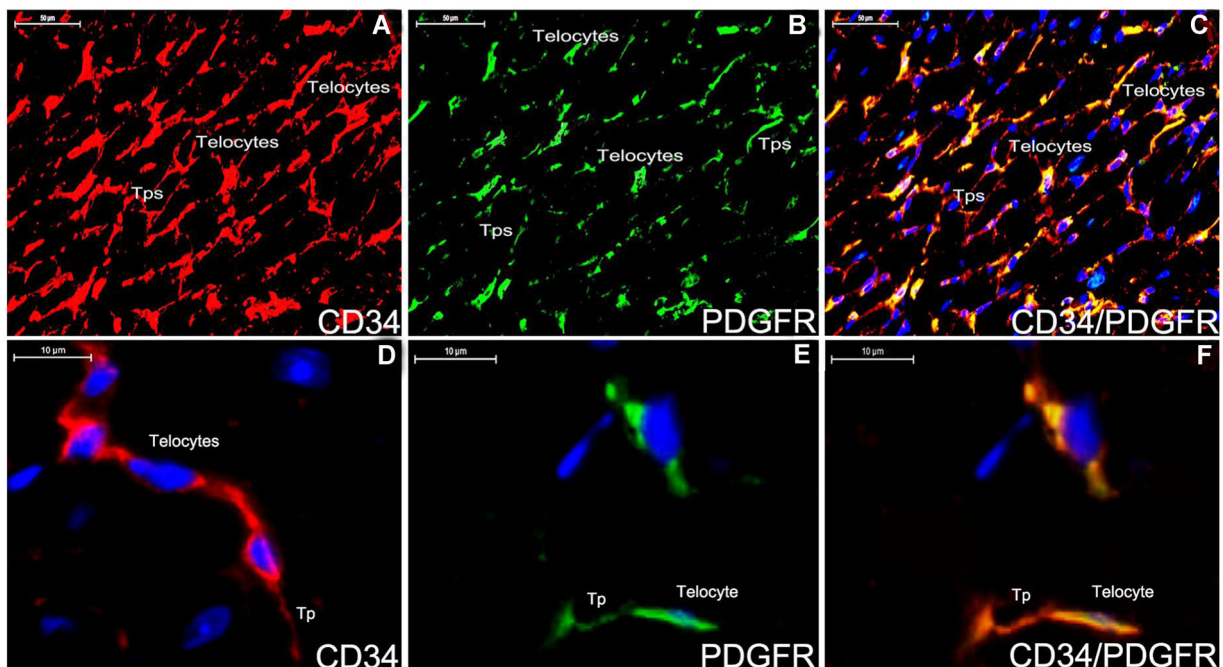


**Figure 2** Double staining immunofluorescence for CD34/PDGFR- $\alpha$  in the myocardium tissue of ApoE<sup>-/-</sup> mice (A-F). The distribution of telocyte is shown positively with CD34 (A,red), PDGFR- $\alpha$  (B,green) and CD34/PDGFR- $\alpha$  (C,yellow). Telocyte can construct a 3D network in the myocardium tissue (A-C). The morphology of telocyte is completely shown (D-F). CD34-positive telocyte is oval-like with two telopodes (D,red). PDGFR- $\alpha$ -positive telocyte is spindle-like with one telopode (E,green). Telocyte expresses for CD34/PDGFR- $\alpha$  (F,yellow). Nuclei were counterstained with DAPI(blue). The scale bar = 50 $\mu$ m (A-C) and 10 $\mu$ m (D-E).

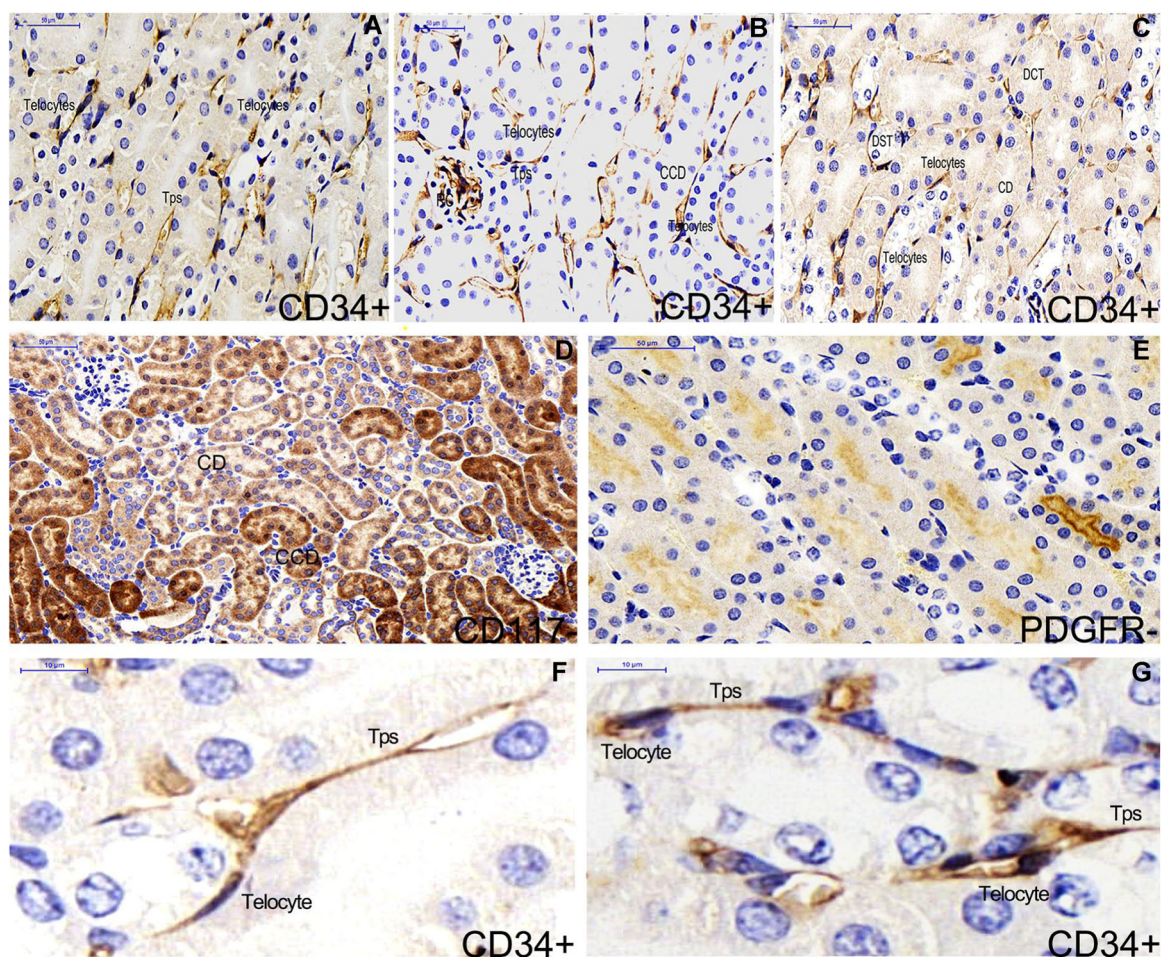


**Figure 3** Single label immunohistochemistry of CD34, CD117 and PDGFR- $\alpha$  in kidney of ApoE<sup>-/-</sup> mice (A-E). CD34-positive telocyte is shown and telocyte morphology are similar in the cortex system (B) and medulla nephrica system (A,C) of renal tissues. Epithelial cells of renal tubular are extensively stained by the CD117 label (D). There is no telocyte shown by CD117 and PDGFR- $\alpha$  label (D,E). The morphology of telocyte is overtly shown in the medulla nephrica system (F) and in the cortex system (G). CCD: cortical collecting duct. RC: renal corpuscle. CD: collecting duct. DCT: distal convoluted tubule. DST: distal straight tubule. Nuclei were counterstained with haematoxylin(blue). The scale bar = 50 $\mu$ m (A-E) and 10 $\mu$ m (F,G).

(Figure 5A-C,E). Telocyte immunophenotypes in the liver parenchyma tissue and hepatic vein system are distinct (Figure 6). No evidence of telocytes for CD28/Vimentin in the liver parenchyma tissue (A-C) and CD34/CD117 in the hepatic vein system (D-F) are detected. CD28/Vimentin and CD34/CD117 double immunofluorescence labels are considered as the negative control (Figure 7).

**Discussion**

Medical studies on telocytes have been conducted for several decades. Recently, the mechanisms of telocyte behaviour Which play a key role in organ's development and diseases attract scientists' attention (Popescu and Faussone-Pellegrini, 2010; Yang et al., 2014; Corradi et al., 2013; Rusu et al., 2014; Bosco et al., 2013).

ApoE<sup>-/-</sup> mice, which are considered the classical animal model of atherosclerosis (AS), has been utilized to identify the relationship between genetic deficiency and hyperlipidaemia in humans. The ApoE gene is the most basic and significant risk factor in the procession of atherosclerotic vessels under high fat diets in the mammals (Rinne et al., 2018; Sfyriand and Matsakas, 2017). To identify the evidence of telocytes in the pathophysiology of atherosclerosis, our study confirmed the morphology and biochemical characteristics of telocyte in vital organs of ApoE<sup>-/-</sup> mice, and identified that biochemical markers could express the normal configuration of telocyte which was as the same as it in the wild type mice (Xiao et al., 2013).

Many techniques have been used to study telocytes in situ and in vitro. TEM has always been the “gold standard” method

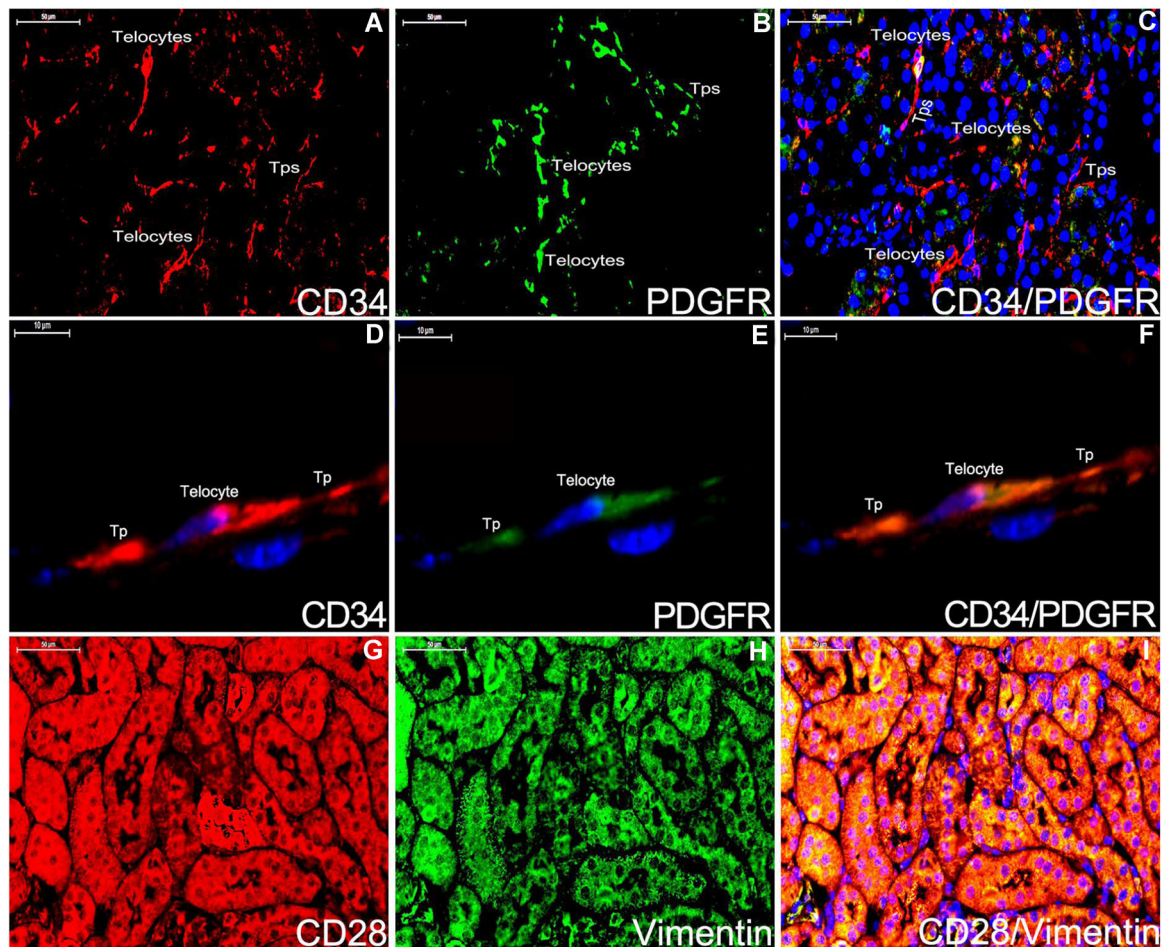


**Figure 4** Double staining immunofluorescence for CD28/Vimentin and CD34/PDGFR- $\alpha$  in kidney of ApoE<sup>-/-</sup> mice (A-I). CD34-positive telocyte and telopode are integrally shown (A,D;red). The partial section of telocytes and telopodes express PDGFR- $\alpha$  (B,E;green). CD34/PDGFR- $\alpha$  are displayed positively for telocyte and telopode (C,F;yellow). CD28 and Vimentin staining are considered as the negative control for telocyte (G-I). Nuclei were counterstained with DAPI(blue). The scale bar = 50 $\mu$ m (A-C;G-I) and 10 $\mu$ m (D-F).

to distinguish telocytes from other interstitial cells and epithelial cell (Cantarero et al., 2016). Immunohistochemistry and immunofluorescence assays are other common and crucial techniques to observe the distribution, origination and function of telocytes (Zhou et al., 2010). Telocytes represent various immunohistochemical bio-markers in different organs, including CD117, CD34, Vimentin, caveolin-1, platelet-derived growth factor receptor- $\alpha$  (PDGFR- $\alpha$ ), vascular endothelial growth factor (VEGF), and inducible nitric oxide synthase (iNOS) (Popescu et al., 2010; Suciuc et al., 2012; Petre et al., 2016; Chang et al., 2015; Vannucchi et al., 2013). Wagener showed that the telocyte in bovine teat sphincters expressed CD117 (Rusu et al., 2012) and Vimentin (Wagener et al., 2018). Telocytes in a cytology study of the cardiovascular system were found to co-express CD117, CD34, Vimentin, nestin and S-100 in the epicardium. Furthermore, telocytes were positive for CD117, CD34, Vimentin and EGFR and negative for nestin,

desmin, CD13 and S-100 in the myocardium (Hinescu et al., 2006). In our studies, telocytes were verified to be positive for CD117, PDGFR- $\alpha$  and CD34, as well as, negative for CD28 in the heart and liver organ. Telocytes were positive for CD34 and PDGFR- $\alpha$ , and negative for CD117 in the cortex system and medulla nephrica system of kidney.

Moreover, telocytes and stem/progenitor cells were demonstrated to derive from the mesenchy cell niche and have the same presentation of immunophenotype CD34 positive in the epicardium, lungs, skeletal muscle, choroid plexus, skin and liver organs (Popescu and Nicolescu, 2013; Cantarero et al., 2011). The accurate method to differentiate the stem cell and telocytes is the transmitted electron microscopy and the scanning electron microscopy that ultrastructure and morphology of cells can be effortlessly manifested, but immunohistochemistry technique is another critical way to distinguish cells on the basis of the distinct

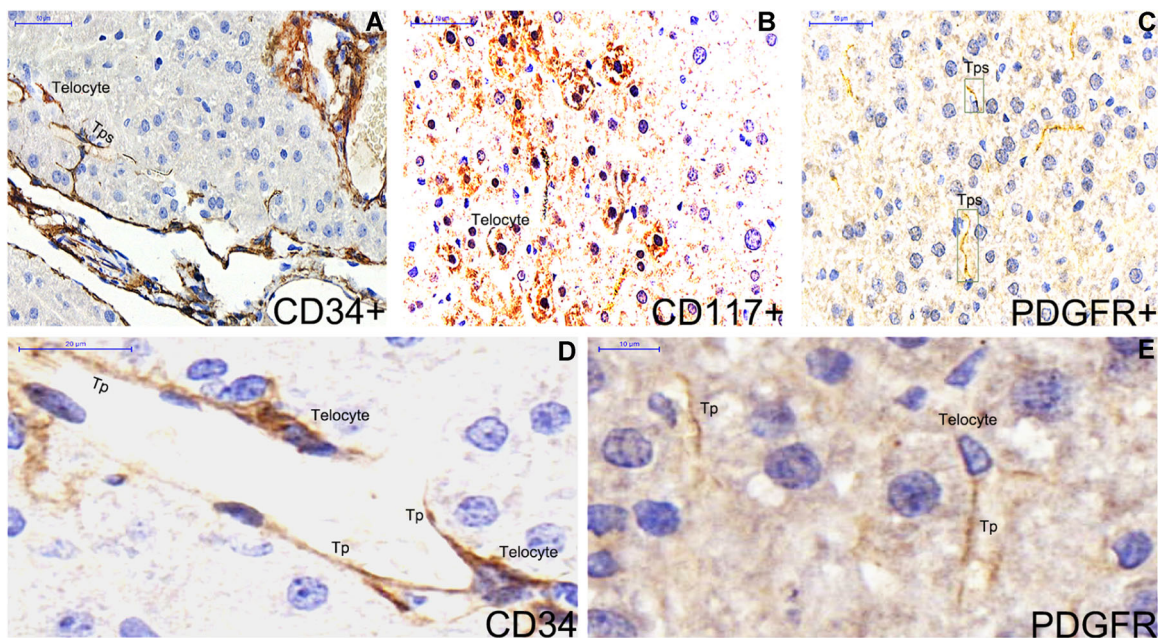


**Figure 5** Single label immunohistochemistry for CD34, CD117 and PDGFR- $\alpha$  are stained in liver of ApoE<sup>-/-</sup> mice (A-E). CD34-positive telocytes with five prolonged and thin telopodes are stelliform adjacent the hepatic sinusoid (A,D). CD117 is distributed like spots in the hepatocyte area. CD117-positive telocytes are observed among hepatocytes (B). Telopode is positively stained for PDGFR- $\alpha$  (C,E). Nuclei were counterstained with haematoxylin(blue). The scale bar = 50 $\mu$ m (A-C) and 10 $\mu$ m (D-E).

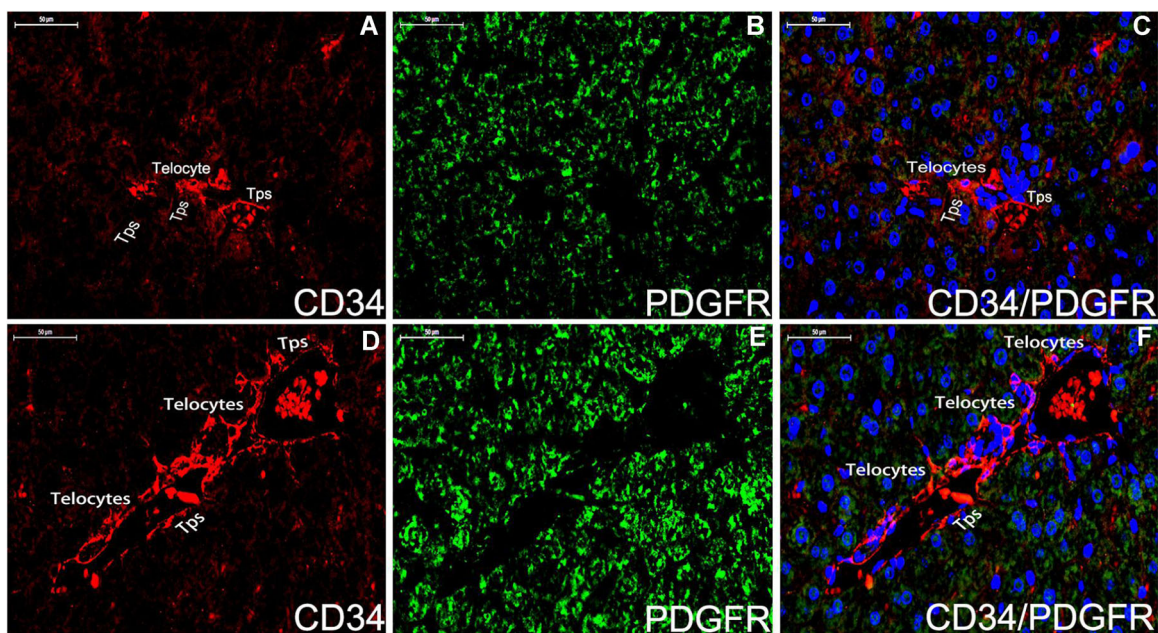


**Figure 6** Double staining immunofluorescence for CD34/PDGFR- $\alpha$  in the liver parenchyma tissue (A-C) and hepatic vein system (D-F). In the liver parenchyma tissue, CD34-positive(red) telocytes with telopodes are expressed (A,C), and telocyte is negative for PDGFR- $\alpha$  (B,green). In the hepatic vein system, telocytes and telopodes positive for CD34 are observed around vascular wall of hepatic vein (D,red) but it is difficult to distinguish telocytes for PDGFR- $\alpha$  (E,green). Nuclei were counterstained with DAPI(blue). The scale bar = 50 $\mu$ m. Tps: telopodes.

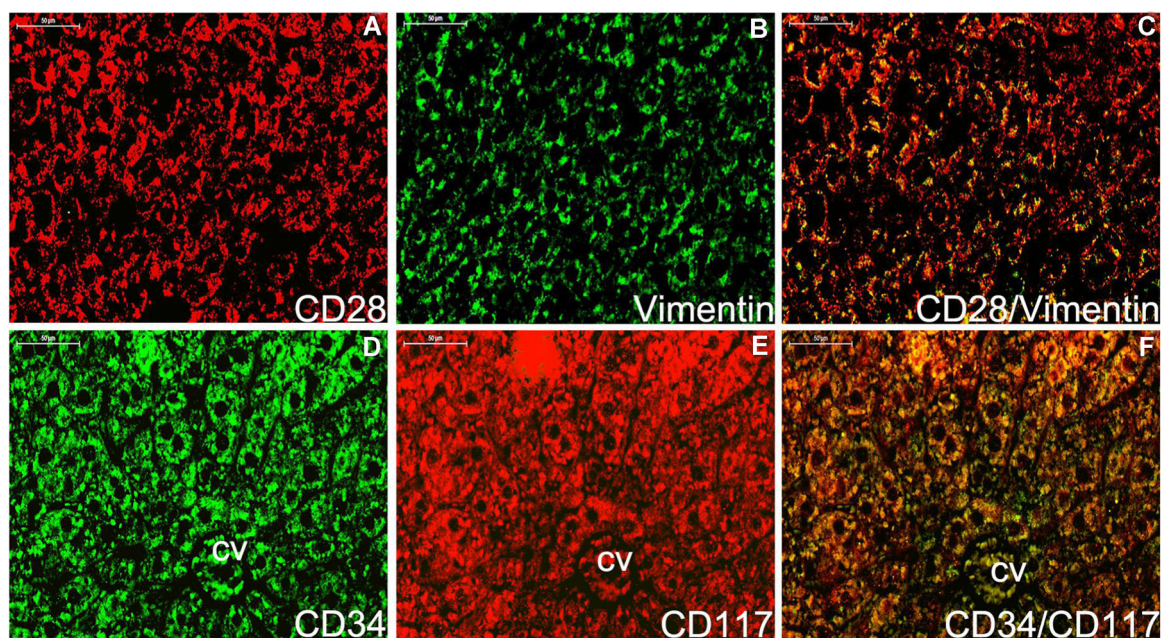


**Figure 7** Double staining immunofluorescence for CD28/Vimentin and CD34/CD117 in the liver (A-F). No evidence of telocytes for CD28/Vimentin in the liver parenchyma tissue (A-C) and CD34/CD117 in the hepatic vein system (D-F) are detected. CD28/Vimentin and CD34/CD117 double immunofluorescence labels are considered as the negative control. Nuclei were counterstained with DAPI (blue). The scale bar = 50µm.

morphology after bio-marker stained, such as CD34 positive telocytes with several prolonged and moniliform feature called telopodes are different from CD34 positive stem/progenitor cells which only express an elliptic or cycloidal cell body without stromal synapses in the same tissue.

Telocytes have been discovered to participate in the pathophysiological process of regeneration and repair of a tissue while it suffers from injury, infection and apoptosis so that telopodes, deriving from the body of telocytes and possessing the identical cytoplasm which constitutes of enormous organelles and ribonucleoprotein, are recognized as the ligament of intercellular communications with neighbouring cells. Furthermore, telocytes can form a three-dimension network during the development of a new tissue and be proved to disappear when organs are subject to be dysfunction. Therefore, telocytes have “strategic” position in ambient cells’ contact and play a key role in the signal transfer.

## Conclusions

Telocytes have been implicated in regeneration (Gherghiceanu and Popescu, 2012), repair (Gherghiceanu and Popescu, 2012; Sadri *et al.*, 2016; Akram *et al.*, 2016), homeostasis (Cretoi *et al.*, 2009), intercellular signalling (Gherghiceanu and Popescu, 2011), and angiogenesis (Manole *et al.*, 2011) in humans and animals. In future studies, we will use TEM to determine the ultrastructure of telocytes and culture telocytes *in vitro* to profile the genetic information of related extracellular vesicles and signalling proteins.

*in vitro* to profile the genetic information of related extracellular vesicles and signalling proteins.

## Acknowledgement

We thank all boffin in Medical Research Center of Shandong Provincial Qianfoshan Hospital. The research is supported by grants from Key Research and Development Plan of Shandong Province (No. 2016GSF201108) and Shandong Natural Science Foundation (No. ZR2019MH116).

## Conflict of interest

The authors declare that there are no conflicts of interest.

## Ethical approval

All procedures performed in studies involving animals were in accordance with the ethics committee of Shandong Provincial Qianfoshan Hospital affiliated to Shandong University and the ethics approval number is S95.

## References

- Akram K, Patel N, Spiteri M, Forsyth N (2016) Lung Regeneration: Endogenous and Exogenous Stem Cell mediated therapeutic approaches. *Int J Mol Sci* 17(1) <https://doi.org/10.3390/ijms17010128>

- Alunno A, Ibba-Manneschi L, Bistoni O, Rosa I, Caterbi S, Gerli R, Manetti M (2015) Telocytes in minor salivary glands of primary Sjogren's syndrome: association with the extent of inflammation and ectopic lymphoid neogenesis. *J Cell Mol Med* 19(7): 1689–96. <https://doi.org/10.1111/jcmm.12545>
- Bode F, Blanck O, Gebhard M, Hunold P, Grossherr M, Brandt S, Rades D (2015) Pulmonary vein isolation by radiosurgery: implications for non-invasive treatment of atrial fibrillation. *Europace* 17(12): 1868–74. <https://doi.org/10.1093/europace/euu406>
- Bosco C, Diaz E, Gutierrez R, Gonzalez J, Perez J (2013) Ganglionic nervous cells and telocytes in the pancreas of Octodon degus: extra and intrapancreatic ganglionic cells and telocytes in the degus. *Auton Neurosci* 177(2): 224–30. <https://doi.org/10.1016/j.autneu.2013.05.002>
- Cantarero Carmona I, Luesma Bartolome MJ, Junquera Escribano C (2011) Identification of telocytes in the lamina propria of rat duodenum: transmission electron microscopy. *J Cell Mol Med* 15(1): 26–30. <https://doi.org/10.1111/j.1582-4934.2010.01207.x>
- Cantarero I, Luesma MJ, Alvarez-Dotu JM, Munoz E, Junquera C (2016) Transmission Electron Microscopy as Key Technique for the Characterization of Telocytes. *Curr Stem Cell Res Ther* 11(5): 410–14. <https://doi.org/10.2174/1574888X10666150306155435>
- Cantarero I, Luesma MJ, Junquera C (2011) The primary cilium of telocytes in the vasculature: electron microscope imaging. *J Cell Mol Med* 15: 2594–600. <https://doi.org/10.1111/j.1582-4934.2011.01312.x>
- Chang Y, Li C, Gan L, Li H, Guo Z (2015) Telocytes in the Spleen. *PLoS One* 10(9): e0138851. <https://doi.org/10.1371/journal.pone.0138851>
- Corradi LS, Jesus MM, Fochi RA, Vilamaior PS, Justulin LA, Jr., Goes RM, Taboga SR (2013) Structural and ultrastructural evidence for telocytes in prostate stroma. *J Cell Mol Med* 17(3): 398–406. <https://doi.org/10.1111/jcmm.12021>
- Cretoiu SM, Cretoiu D, Suci L, Popescu LM (2009) Interstitial Cajal-like cells of human Fallopian tube express estrogen and progesterone receptors. *J Mol Histol* 40(5-6): 387–94. <https://doi.org/10.1007/s10735-009-9252-z>
- Declodt A, Schwarzwald CC, De Clercq D, Van Der Vekens N, Pardon B, Reef VB, van Loon G (2015) Risk factors for recurrence of atrial fibrillation in horses after cardioversion to sinus rhythm. *J Vet Intern Med* 29(3): 946–53. <https://doi.org/10.1111/jvim.12606>
- Gherghiceanu M, Popescu LM (2011) Heterocellular communication in the heart: electron tomography of telocyte-myocyte junctions. *J Cell Mol Med* 15(4): 1005–11. <https://doi.org/10.1111/j.1582-4934.2011.01299.x>
- Gherghiceanu M, Popescu LM (2012) Cardiac telocytes - their junctions and functional implications. *Cell Tissue Res* 348(2): 265–79. <https://doi.org/10.1007/s00441-012-1333-8>
- Gherghiceanu M, Hinescu ME, Andrei F, Mandache E, Macarie CE, Faussonne-Pellegrini MS, Popescu LM (2008) Interstitial Cajal-like cells (ICLC) in myocardial sleeves of human pulmonary veins. *J Cell Mol Med* 12(5a): 1777–81. <https://doi.org/10.1111/j.1582-4934.2008.00444.x>
- Hinescu ME, Gherghiceanu M, Mandache E, Ciotea SM, Popescu LM (2006) Interstitial Cajal-like cells (ICLC) in atrial myocardium: ultrastructural and immunohistochemical characterization. *J Cell Mol Med* 10(1): 243–57. <https://doi.org/10.1111/j.1582-4934.2006.tb00306.x>
- Manole CG, Cismasiu V, Gherghiceanu M, Popescu LM (2011) Experimental acute myocardial infarction: telocytes involvement in neo-angiogenesis. *J Cell Mol Med* 15(11): 2284–96. <https://doi.org/10.1111/j.1582-4934.2011.01449.x>
- Nakashima Y, Plump AS, Raines EW, Breslow JL, Ross R (1994) ApoE-deficient mice develop lesions of all phases of atherosclerosis throughout the arterial tree. *Arterioscler Thromb* 14(1): 133–40.
- Nicolescu MI, Popescu LM (2012) Telocytes in the interstitium of human exocrine pancreas: ultrastructural evidence. *Pancreas* 41(6): 949–56. <https://doi.org/10.1097/MPA.0b013e31823fbded>
- Petre N, Rusu MC, Pop F, Jianu AM (2016) Telocytes of the mammary gland stroma. *Folia Morphol (Warsz)* 75(2): 224–31. <https://doi.org/10.5603/FM.a2015.0123>
- Popescu LM, Faussonne-Pellegrini MS (2010) TELOCYTES - a case of serendipity: the winding way from Interstitial Cells of Cajal (ICC), via Interstitial Cajal-Like Cells (ICLC) to TELOCYTES. *J Cell Mol Med* 14(4): 729–40. <https://doi.org/10.1111/j.1582-4934.2010.01059.x>
- Popescu LM, Manole CG, Gherghiceanu M, Ardelean A, Nicolescu MI, Hinescu ME, Kostin S (2010) Telocytes in human epicardium. *J Cell Mol Med* 14(8): 2085–93. <https://doi.org/10.1111/j.1582-4934.2010.01129.x>
- Popescu LM, Nicolescu MI (2013) Telocytes and stem cells. In: RCdS Goldenberg, & AC Campos deCarvalho eds. *Resident stem cells and regenerative therapy*. 1st ed. Academic Press/Elsevier, pp. 205–31. <http://www.sciencedirect.com/science/article/pii/B9780124160125000116> In: editors Chapter 11. ISBN 9780124160125
- Rinne P, Kadiri JJ, Velasco-Delgado M, Nuutinen S, Viitala M, Hollmen M, Steffens S (2018) Melanocortin 1 Receptor Deficiency Promotes Atherosclerosis in Apolipoprotein E(-/-) Mice. *Arterioscler Thromb Vasc Biol* 38(2): 313–23. <https://doi.org/10.1161/atvbaha.117.310418>
- Rusu MC, Jianu AM, Mirancea N, Didilescu AC, Manoiu VS, Paduraru D (2012) Tracheal telocytes. *J Cell Mol Med* 16(2): 401–05. <https://doi.org/10.1111/j.1582-4934.2011.01465.x>
- Rusu MC, Loreto C, Manoiu VS (2014) Network of telocytes in the temporomandibular joint disc of rats. *Acta Histochem* 116(4): 663–68. <https://doi.org/10.1016/j.acthis.2013.12.005>
- Rusu MC, Mirancea N, Manoiu VS, Valcu M, Nicolescu MI, Paduraru D (2012) Skin telocytes. *Ann Anat* 194(4): 359–67. <https://doi.org/10.1016/j.aanat.2011.11.007>
- Sadri AR, Jeschke MG, Amini-Nik S (2016) Advances in Liver Regeneration: Revisiting Hepatic Stem/Progenitor Cells and

- Their Origin. *Stem Cells Int*, 2016: 7920897–9 <https://doi.org/10.1155/2016/7920897>
- Sfyri P, Matsakas A (2017) Crossroads between peripheral atherosclerosis, western-type diet and skeletal muscle pathophysiology: emphasis on apolipoprotein E deficiency and peripheral arterial disease. *J Biomed Sci* 24(1): 42. <https://doi.org/10.1186/s12929-017-0346-8>
- Suciu LC, Popescu BO, Kostin S, Popescu LM (2012) Platelet-derived growth factor receptor-beta-positive telocytes in skeletal muscle interstitium. *J Cell Mol Med* 16(4): 701–7. <https://doi.org/10.1111/j.1582-4934.2011.01505.x>
- Vandecasteele T, Van Den Broeck W, Tay H, Couck L, van Loon G, Cornillie P (2018) 3D reconstruction of the porcine and equine pulmonary veins, supplemented with the identification of telocytes in the horse. *Anat Histol Embryol* 47(2): 145–52. <https://doi.org/10.1111/ahe.12334>
- Vannucchi MG, Traini C, Manetti M, Ibba-Manneschi L, Fausone-Pellegrini MS (2013) Telocytes express PDGFRalpha in the human gastrointestinal tract. *J Cell Mol Med* 17(9): 1099–108. <https://doi.org/10.1111/jcmm.12134>
- Wagener MG, Leonhard-Marek S, Hager JD, Pfarrer C (2018) CD117- and vimentin-positive telocytes in the bovine teat sphincter. *CD117- and Vimentin-positive telocytes in the bovine teat sphincter* 47(3): 268–70. <https://doi.org/10.1111/ahe.12347>
- Xiao J, Wang F, Liu Z, Yang C (2013) Telocytes in liver: electron microscopic and immunofluorescent evidence. *J Cell Mol Med* 17(12): 1537–42. <https://doi.org/10.1111/jcmm.12195>
- Yang P, Ahmed N, Ullah S, Chen Q, Zheng Y (2016) Features of Telocytes in Agricultural Animals. *Adv Exp Med Biol* 913: 105–13. [https://doi.org/10.1007/978-981-10-1061-3\\_6](https://doi.org/10.1007/978-981-10-1061-3_6)
- Yang Y, Sun W, Wu SM, Xiao J, Kong X (2014) Telocytes in human heart valves. *J Cell Mol Med* 18(5): 759–65. <https://doi.org/10.1111/jcmm.12285>
- Zheng Y, Bai C, Wang X (2012) Telocyte morphologies and potential roles in diseases. *J Cell Physiol* 227(6): 2311–7. <https://doi.org/10.1002/jcp.23022>
- Zhou J, Zhang Y, Wen X, Cao J, Li D, Lin Q, Wang C (2010) Telocytes accompanying cardiomyocyte in primary culture: two- and three-dimensional culture environment. *J Cell Mol Med* 14(11): 2641–5. <https://doi.org/10.1111/j.1582-4934.2010.01186.x>

Received 16 October 2018; accepted 15 March 2019.  
Final version published online 28 June 2019.